Cell Metabolism
Article

Neuron-Derived Semaphorin 3A Is an Early Inducer of Vascular Permeability in Diabetic Retinopathy via Neuropilin-1

Agustin Cerani,[1,2,4] Nicolas Tetreault,[2,3,4] Catherine Menard,[2,4] Eric Lapalme,[1] Chintan Patel,[1] Nicholas Sitaras,[1] Felix Beaudoin,[2] Dominique Leboeuf,[2] Vincent De Guire,[2] François Binet,[1] Agnieszka Dejda,[2] Flavio A. Rezende,[1] Khalil Miloudi,[3] and Przemyslaw Sapieha[1,2,3,*]

[1]Department of Ophthalmology, Maisonneuve-Rosemont Hospital Research Centre, University of Montreal, Montreal, QC H1T 2M4, Canada
[2]Department of Biochemistry, Maisonneuve-Rosemont Hospital Research Centre, University of Montreal, Montreal, QC H1T 2M4, Canada
[3]Department of Neurology-Neurosurgery, McGill University, Montreal, QC H3A 2B4, Canada
[4]These authors contributed equally to this work
*Correspondence: mike.sapieha@umontreal.ca
http://dx.doi.org/10.1016/j.cmet.2013.09.003

SUMMARY

The deterioration of the inner blood-retinal barrier and consequent macular edema is a cardinal manifestation of diabetic retinopathy (DR) and the clinical feature most closely associated with loss of sight. We provide evidence from both human and animal studies for the critical role of the classical neuronal guidance cue, semaphorin 3A, in instigating pathological vascular permeability in diabetic retinas via its cognate receptor neuropilin-1. We reveal that semaphorin 3A is induced in early hyperglycemic phases of diabetes within the neuronal retina and precipitates initial breakdown of endothelial barrier function. We demonstrate, by a series of orthogonal approaches, that neutralization of semaphorin 3A efficiently prevents diabetes-induced retinal vascular leakage in a stage of the disease when vascular endothelial growth factor neutralization is inefficient. These observations were corroborated in $Tg^{Cre\text{-}Esr1}/Nrp1^{flox/flox}$ conditional knockout mice. Our findings identify a therapeutic target for macular edema and provide further evidence for neurovascular crosstalk in the pathogenesis of DR.

INTRODUCTION

Diabetic retinopathy (DR) is the most prominent complication of diabetes and the leading cause of blindness in working-age individuals (Kempen et al., 2004). It is characterized by an initial microvascular degeneration followed by a compensatory but pathological hypervascularization mounted by the hypoxic retina in an attempt to reinstate metabolic equilibrium (Cheung and Wong, 2008; Sapieha, 2012). Although often initially asymptomatic, loss of sight is provoked primarily by diabetic macular edema (DME), vitreous hemorrhages, and in advanced cases, preretinal neovascularization and tractional retinal detachment (Antonetti et al., 2012; Wang et al., 2012). Of these, DME is the most common cause of central vision loss in diabetics, affecting over 25% of patients suffering from diabetes (Moss et al., 1998). It is triggered secondary to the deterioration of the blood-retinal barrier (BRB) and the consequent increase in extravasation of fluids and plasma components into the vitreous cavity. Ultimately, the decrease in retinal vascular barrier function leads to vasogenic edema and pathological retinal thickening.

Although significant effort has been invested in elucidating the mechanisms that govern destructive preretinal neovascularization in DR (Silva et al., 2010; Stahl et al., 2010; Wang et al., 2012), considerably less is known about the cellular processes that lead to increased retinal vascular permeability. Moreover, current standards of care present non-negligible side effects. These include increased cataract formation and a harmful rise in intraocular pressure with intravitreal use of corticosteroid (Silva et al., 2010). Similarly, anti-VEGF (vascular endothelial growth factor) therapies, which in general exhibit respectable safety profiles, may be associated with increased thromboembolic events (Stewart, 2012), possible neuronal toxicity (Foxton et al., 2013; Robinson et al., 2001; Saint-Geniez et al., 2008), and geographic atrophy (Martin et al., 2011; 2012) when used as frequent long-term regimens. Moreover, the first and most widely used form of treatment is panretinal photocoagulation, for either proliferative diabetic retinopathy (PDR) or grid/focal laser for DME. Laser-based photocoagulation approaches destroy hypoxic retinal tissue secreting proangiogenic factors and inadvertently lead to reduced visual field or central or paracentral scotomas. These therapeutic limitations highlight the need for novel pharmacological interventions.

Current investigations into the molecular mechanisms that cause DME have largely focused on VEGF. This may be attributed in part to the fact that the prominent clinical features of DR have led to the general inference that it is entirely of a microvascular nature. Yet, evidence points to early changes in the neural retina (Kern and Engerman, 1996; Barber et al., 1998; 2005; Gastinger et al., 2008). While there is irrefutable evidence for a neurovascular link in the progression of DR (Antonetti et al., 2012), neurovascular crosstalk has received limited attention in the context of DR pathogenesis. Consistent with a breakdown in neurovascular crosstalk in ischemic retinopathies, we have recently shown that semaphorin 3A (SEMA3A), a classic neuronal guidance cue that also affects endothelial cell behavior, is produced by stressed retinal ganglion cells (RGCs) and

partakes in deviating neovessels toward physiologically avascular regions of the eye (Joyal et al., 2011).

In neurons, binding of SEMA3A to its cognate receptor neuropilin-1 (NRP1) provokes cytoskeletal collapse via plexins (Takahashi et al., 1999); the transduction mechanism in endothelial cells remains ill defined (Gelfand et al., 2009). Neuropilin-1 has the particular ability to bind two structurally dissimilar ligands via distinct sites on its extracellular domain (Gluzman-Poltorak et al., 2001; Lee et al., 2002; Mamluk et al., 2002). It binds SEMA3A (Klagsbrun and Eichmann, 2005; Miao et al., 1999), provoking cytoskeletal collapse and $VEGF_{165}$ (Gluzman-Poltorak et al., 2001; Klagsbrun and Eichmann, 2005; Klagsbrun et al., 2002; Mamluk et al., 2002), enhancing binding to VEGFR2, and thus increasing its angiogenic potential (Soker et al., 2002). Crystallographic evidence revealed that $VEGF_{165}$ and Sema3A do not directly compete for Nrp1, but rather can simultaneously bind to Nrp1 at distinct, nonoverlapping sites (Appleton et al., 2007). Moreover, genetic studies show that NRP1 distinctly regulates the effects of VEGF and SEMA3A on neuronal and vascular development (Vieira et al., 2007). Notably, it was proposed that, similar to VEGF, Sema3A may itself promote vascular permeability (Acevedo et al., 2008); this is a counterintuitive observation, given the divergent biological roles of VEGF and Sema3A. However, the role of Sema3A in mediating the breakdown of barrier function, such as that observed in diabetic retinopathy, has not been explored to date.

Here we provide evidence for the role of a neuron-derived guidance cue (Sema3A) in disrupting retinal barrier function in diabetic retinopathy. We demonstrate in both human patients and animal models that ocular Sema3A is robustly induced in the early stages of diabetes and mediates, via NRP1, the breakdown of the inner BRB. Neutralizing Sema3A may represent an attractive alternative therapeutic strategy to counter pathologic vascular permeability in DR.

RESULTS

Sema3A Is Elevated in the Vitreous of Human Patients Suffering from Diabetic Retinopathy

In order to evaluate the potential role of Sema3A in mediating the edematous phenotype observed in DR, we first sought to determine the presence of this guidance cue in the vitreous of patients suffering from DME. Vitreous was recovered during standard vitroretinal surgery from 21 patients. Ten samples were obtained from patients suffering from DME and 11 from control patients (nonvascular pathology) undergoing surgery for macular hole (MH) or epiretinal membrane (ERM) (Table 1). Spectral-domain optical coherence tomography (SD-OCT) was performed, and three-dimensional (3D) retinal maps were generated to evaluate the extent of retinal damage and edema. In contrast to controls, sampled DME patients showed significant retinal swelling, specifically in the macular and perimacular zones (Figures 1A–1D).

Consistent with a prospective role in DME, ELISA-based detection of Sema3A revealed a significant increase in the vitreous of patients suffering from DME when compared to nonvascular ocular pathologies (control median 3.79 ng/ml [interquartile range {IQR}: 25%, 75%: 2.08 ng/ml, 5.58 ng/ml]; DME median 16.27 ng/ml [IQR: 25%, 75%: 5.770 ng/ml, 35.36 ng/ml]; $p = 0.0464$) (Figure 1E). Western blot analysis of vitreous from patients corroborated data obtained by ELISA and revealed that Sema3A (~125 kDa and ~95kDa) (Klebanov et al., 2009; Koppel and Raper, 1998) was robustly induced in most patients affected by DME (Figure 1F). Specificity of the α-Sema3A antibody employed was verified by shRNA-mediated knockdown of *Sema3A* in human cells expressing high levels of endogenous Sema3A (HeLa) and by immunoblotting serially diluted recombinant Sema3A protein (Figure S1 available online). Detailed patient characteristics are presented in Table 1. These data on human subjects provide the rationale to explore the role of Sema3A in the context of diabetes-induced BRB breakdown.

Table 1. Characteristics of Patients Having Undergone Vitreous Biopsy

Sample	Age (Years)	Db Type	Duration (Years)	Retinopathy	Analysis
C1	65	NA	NA	ERM	WB/ELISA
C2	74	NA	NA	MH	WB/ELISA
C3	63	NA	NA	MH	WB
C4	71	NA	NA	MER	WB
C5	78	NA	NA	other	WB
C6	59	NA	NA	MH	ELISA
C7	52	NA	NA	MH	ELISA
C8	59	NA	NA	MH	ELISA
C9	69	NA	NA	ERM	ELISA
C10	54	NA	NA	ERM	ELISA
C11	68	NA	NA	ERM	ELISA
DME1	74	2	2	DME	WB/ELISA
DME2	75	2	10	DME	WB/ELISA
DME3	69	2	20	DME	WB/ELISA
DME4	49	2	3	DME	WB/ELISA
DME5	74	2	15	DME	WB/ELISA
DME6	76	2	30	DME	WB/ELISA
DME7	81	2	–	DME	WB/ELISA
DME8	74	2	15	DME	WB
DME9	62	2	22	DME	ELISA
DME10	63	2	23	DME	ELISA

Demographics of patients selected for vitreous biopsy. Vitreous samples were obtained from 11 controls (nonvascular pathology) and 10 DME patients and analyzed by western blot and ELISA. C, control (nonvascular pathology); Db, diabetes; DME, diabetic macular edema; ERM, epiretinal membrane; MH, macular hole; NA, not applicable; WB, western blot.

Neuronal SEMA3A Is Upregulated in the Early Phases of Streptozotocin-Induced Diabetes

Given the elevated levels of Sema3A in the vitreous of DME patients, we sought to elucidate the dynamics and pattern of *Sema3A* expression in a mouse model of type 1 diabetes mellitus (T1DM). Streptozotocin (STZ) was administered over 5 consecutive days to ~6-week-old C57BL/6J mice, and glycemia was monitored according to the scheme depicted in Figure 2A (modified from Xu et al., 2001). Mice were considered diabetic if their nonfasted glycemia was higher than 17 mM (300 mg/dl).

As early as 4 weeks after induction of diabetes, retinal levels of Sema3A were over 2-fold higher in STZ-treated mice when compared to vehicle-injected controls, while VEGF levels

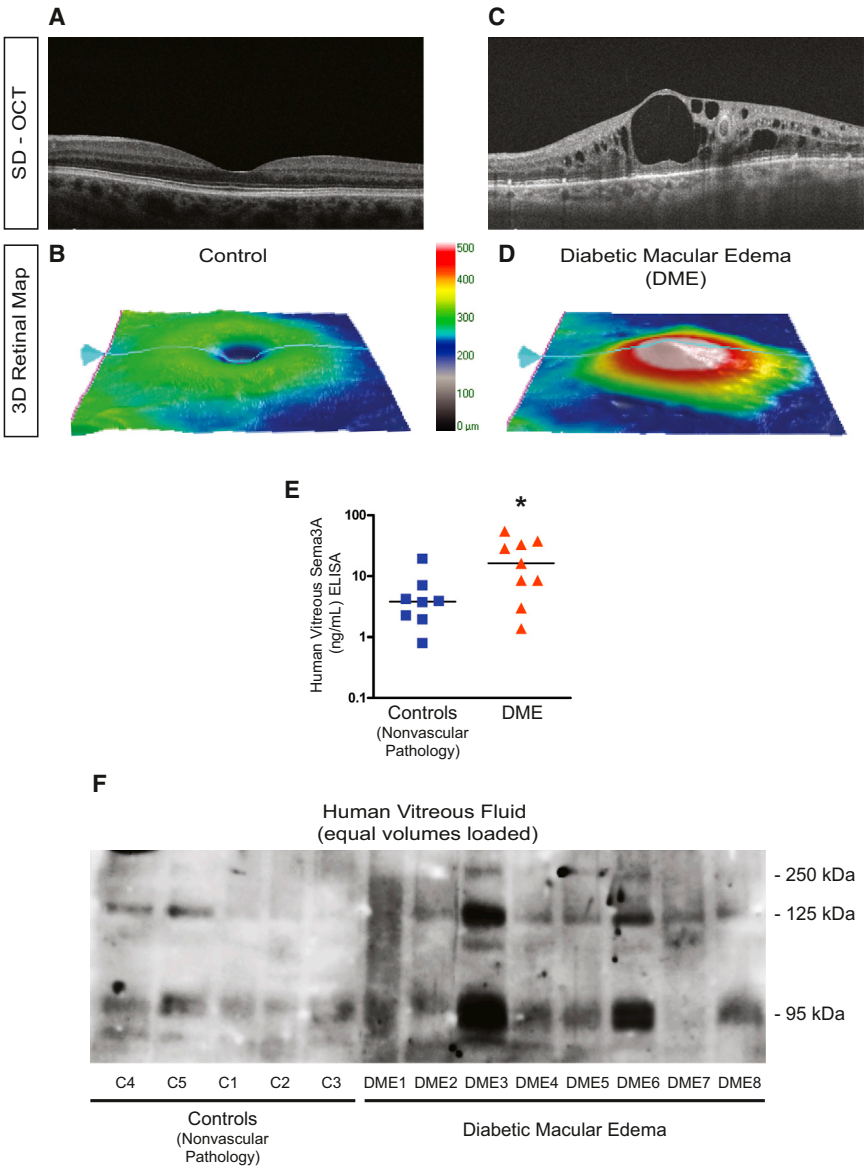

Figure 1. Sema3A Is Elevated in the Vitreous of Human Diabetic Patients Suffering from Diabetic Retinopathy

(A and B) Spectral domain optical coherence tomography (SD-OCT) (A) and 3D retinal maps from healthy eyes (B).

(C and D) In patients suffering from DME, significant retinal swelling (C) mostly in the macular and perimacular zones was noted (D).

(E) ELISA of vitreous humor for Sema3A from control patients with nonvascular pathology and patients suffering from DME. Horizontal lines represent medians for each group.

(F) Western blot analysis of equal volumes of vitreous humor revealed a pronounced induction of Sema3A (~125 kDa and 95 kDa) in a number of patients suffering from DME. See Figure S1 for antibody specificity.

remained unchanged (mean fold increase over control ± SEM: *Sema3A*, 2.234 ± 0.214; p = 0.0045; *Vegf*, 1.123 ± 0.192; p = 0.559, n = 5) (Figure 2B). Significantly higher retinal levels of *Sema3A* persisted at 8 weeks (*Sema3A*, 2.80 ± 0.340; p = 0.0011; *Vegf*, 1.236 ± 0.193; p = 0.266, n = 8), 12 weeks (*Sema3A*, 4.07 ± 0.798; p = 0.00846; *Vegf*, 0.923 ± 0.145; p = 0.612, n = 4), and 14 weeks (*Sema3A*, 2.44 ± 0.593; p = 0.0334; *Vegf*, 3.26 ± 0.65; p = 0.0253, n = 3). Importantly, throughout the early time points of diabetes, VEGF levels in STZ-treated mice remained at similar levels to that observed in vehicle-treated littermates, as has been previously described (Mima et al., 2012), and only started to increase at 14 weeks. The rise in retinal SEMA3A in diabetic mice was confirmed by western blotting at 8 and 14 weeks (Figure 2C). As expected, at all analyzed time points, STZ-treated mice showed pathologically elevated blood glucose levels of ~30 mM for both 4 weeks (citrate, 10.36 ± 0.2935; STZ, 28.81 ± 2.204; p < 0.0001, n = 7) and 8 weeks of diabetes (citrate, 10.72 ± 0.3030; STZ, 27.70 ± 1.780; p < 0.0001, n = 11) (Figure 2D). To corroborate that the observed rise in retinal SEMA3A was provoked by the diabetic state of mice and not STZ toxicity, we investigated retinal *Sema3A* expression in leptin-receptor-deficient (*db/db*) mice, which are a model of type 2 diabetes mellitus (Sapieha et al., 2012). At 24 weeks of life, *db/db* mice showed a 2.5-fold increase in levels of retinal *Sema3A* mRNA when compared to heterozygous *db/+* controls (2.5 ± 0.05; p = 0.0013, n = 3). These data suggest that *Sema3A* was induced as a consequence of diabetes and not off-target effects of STZ (Figure S2).

Importantly, the rise in *Sema3A* expression was an early event in pathogenesis, as it preceded pericyte loss, because both STZ- and vehicle-treated mice showed no significant difference in transcript levels for pericyte markers platelet-derived growth factor receptor-β (*Pdgfr-β*; 1.477 ± 0.364; p = 0.219, n = 11), NG2 proteoglycan (*Ng2*; 2.065 ± 0.886; p = 0.316, n = 4), or alpha smooth muscle actin (*α-Sma*; 1.342 ± 0.441; p = 0.494, n = 4) (Figure 2E). Similarly, immunofluorescence on retinal flatmounts from control and STZ animals confirmed similar vascular coverage by NG2 and SMA-expressing pericytes (Figures 2F–2I).

We next investigated the cellular localization of SEMA3A in the diabetic mouse retina. Immunofluorescence on retinal cryosections revealed that SEMA3A was strongly expressed by retinal neurons of the ganglion cell layer (GCL) (Figures 2J and 2K). Colocalization with the RGC marker βIII-tubulin confirmed that SEMA3A localized to retinal ganglion cells (RGCs) within the diabetic retina (Figure 2K, inset). Consistent with this retinal immunolocalization, laser-capture microdissection of the retinal

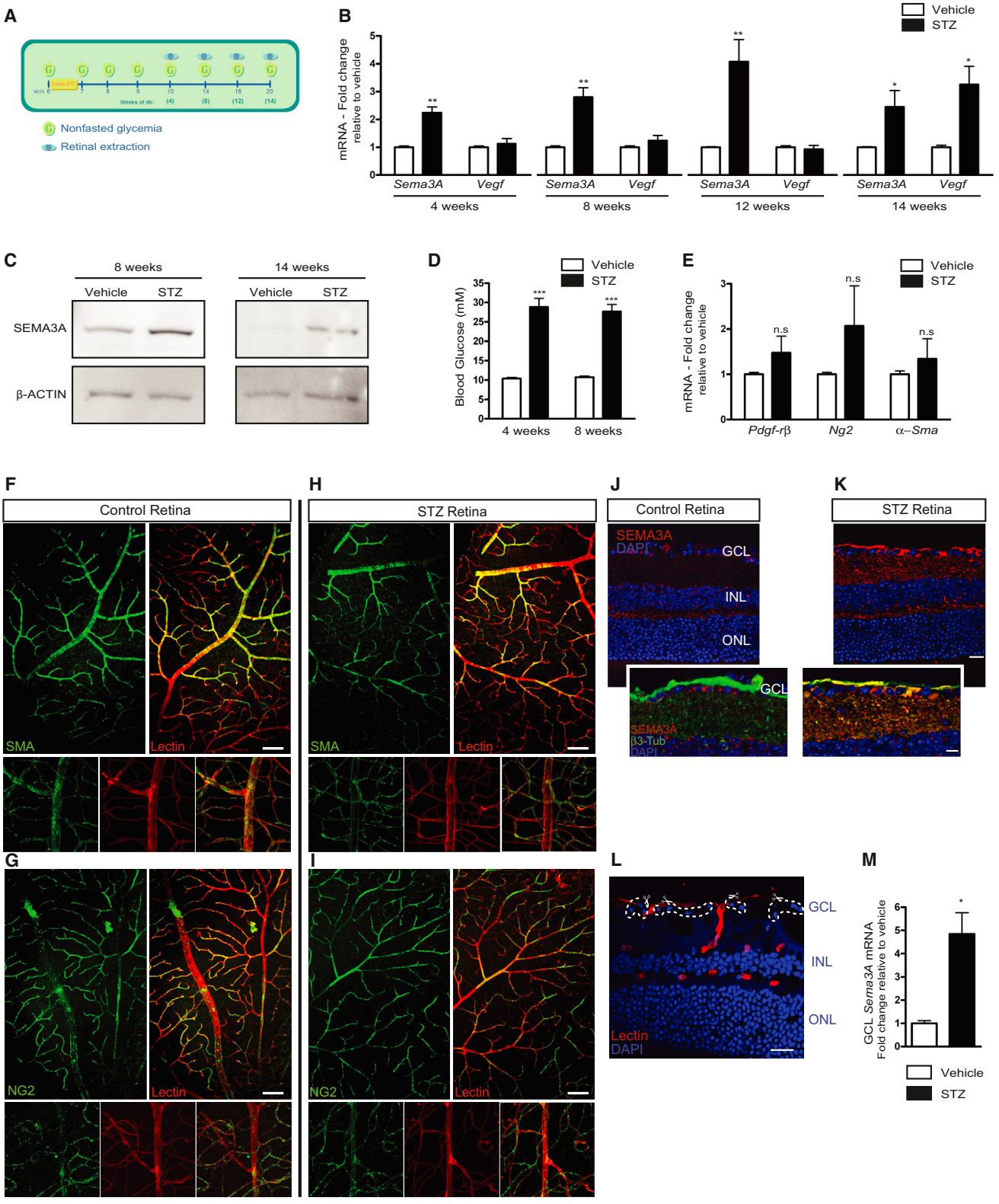

Figure 2. Neuronal *Sema3A* Is Upregulated in the Early Phases of Streptozotocin-Induced Diabetes

(A) Streptozotocin (STZ) was administered to ~6-week-old C57BL/6J mice, and glycemia was monitored according to scheme; a mouse with nonfasted glycemia higher than 17 mM (300 mg/dl) was considered diabetic.

(legend continued on next page)

ganglion cell layer from normal and diabetic mice followed by quantitative RT-PCR revealed an ~5-fold increase of *Sema3A* transcript in RGCs from STZ retinas when compared to age-matched nondiabetic controls (4.848 ± 0.9178; p = 0.014, n = 3) (Figures 2L and 2M). These data provide evidence for the local production of SEMA3A by diabetic neurons in close proximity to the retinal vascular plexus and agree with a role for SEMA3A in mediating the vascular phenotype associated with DME and PDR.

Retinal Barrier Function Is Compromised by SEMA3A

Given the increase in levels of retinal Sema3A observed in the vitreous samples of patients with DME and SEMA3A in mouse retinas in the early stages of diabetes (Figure 2), we proceeded to investigate the propensity of Sema3A to disrupt vascular barrier function. We tested concentrations of Sema3A detected in the vitreous of patients with DME (Figure 1). Because we are assessing acute retinal vascular permeability at 24 hr postinjection and not a protracted effect as would be expected in actual human DME, the tested concentrations of Sema3A were ascending from the pathophysiological levels detected in Figure 1. Retinal vascular permeability was determined by Evans blue (EB) permeation after a single intravitreal injection of Sema3A into adult mouse eyes. Vascular leakage augmented step-wise with increasing concentrations of Sema3A. The increase in vascular leakage reached significance at 25 ng/ml of Sema3A and rose thereafter (mean fold increase over vehicle control ± SEM: 25 ng/ml, 1.302 ± 0.005; p = 0.0003; 50 ng/ml, 1.648 ± 0.059; p = 0.0082; 100 ng/ml, 2.21 ± 0.140; p = 0.0131; 200 ng/ml, 2.57 ± 0.0967; p = 0.0038) (Figure 3A). Concordantly, wet weights of retinas were measured directly upon removing the retina from the eyecup and increased with higher concentrations of intravitreal Sema3A (Figure S3). In order to compare the magnitude of Sema3A-induced retinal vascular permeability with that of VEGF, we scaled the doses to concentrations of VEGF previously reported to induce vascular permeability in murine models (Acevedo et al., 2008) and corrected for molarity. A single intravitreal injection of $VEGF_{165}$ (50 ng/μl) induced a similar magnitude of permeability (1.801 ± 0.0934; p < 0.01) as Sema3A (100 ng/μl; 2.136 ± 0.392; p < 0.05) or a combination of both Sema3A and VEGF (2.258 ± 0.411; p < 0.05) (Figure 3B). Notably, the scaled doses provoked an increase in retinal vascular permeability similar to those of lower concentration (Figure 3A), suggesting a maximal response of Sema3A-induced retinal permeability at lower concentrations. Each dose in Figures 2A and 2B was tested in three distinct experiments with a total of nine mice each.

The propensity of Sema3A to induce vascular leakage was corroborated by confocal imaging of retinal sagittal sections where increased EB permeation (red) throughout the retina signifies elevated plasma albumin extravasation and translates into increased retinal edema (Figure 3C). Notably, with an intravitreal injection of Sema3A, compromised barrier function was also noted in choroidal vessels in addition to retinal vessels. While the mouse retina does not have a macula proper, the observed Sema3A-mediated retinal plasma extravasation taken with the elevated vitreal levels of Sema3A in human patients (Figure 1) are suggestive of a role in mediating loss of barrier function in DME.

Further evidence for the ability of Sema3A to compromise endothelial barrier function was obtained from real-time analysis of transendothelial electric resistance (Murakami et al., 2008) (Figures 3D and 3E). Treatment of an intact monolayer of human umbilical vein endothelial cells (HUVECs) with Sema3A reduced endothelial monolayer impedance (measured from an interval between 3.26 hr and 6 hr; 0.048 > p > 0.009; n = 3) and hence provoked a drop in barrier function in the first 6 hr by a magnitude similar to, yet lower than, VEGF (measured from an interval between 1.12 hr and 6 hr; 0.045 > p > 0.001; n = 4) (Figure 3D).

We next proceeded to determine if Sema3A activated classical signaling pathways that have reported roles in promoting vascular permeability. In this respect, we investigated (by western blot analysis) the activation profiles of Src and focal adhesion kinase (FAK) that are known to transduce extracellular signals that provoke the loosening of endothelial cell junctions (Acevedo et al., 2008; Eliceiri et al., 1999; Scheppke et al., 2008) (Figure 3F). Stimulation of human retinal microvascular endothelial cells (HRMECs) by either Sema3A (100 ng/ml) or VEGF (50 ng/ml) lead to robust phosphorylation of Src at Tyr416 in the activation loop of the kinase domain, which is reported to enhance enzyme activity (Hunter, 1987) (Figure 3G). In turn, FAK was phosphorylated on Tyr576 and Tyr577 (sites for Src kinases) (Figure 3H). Ultimately, the adherens junction protein vascular endothelial (VE)-cadherin became phosphorylated on Tyr731, which is a posttranslational modification associated with increased vascular permeability (Potter

(B) At 4 weeks after induction of diabetes, retinal *Sema3A* mRNA levels rose more than 2-fold in STZ-treated mice when compared to vehicle-injected controls (p = 0.0045, n = 5), ~3-fold at 8 weeks (p = 0.0011, n = 8), 4-fold at 12 weeks (p = 0.00846, n = 4), and ~2.5 fold at 14 weeks (p = 0.0334, n = 3). Conversely, VEGF levels remained unchanged until 14 weeks, at which point they rose by ~3-fold (p = 0.0253, n = 3). Data are represented as mean ± SEM.

(C) Western blot analysis of retinas confirmed that protein levels of SEMA3A were elevated in diabetic mice. See Figure S1 for antibody specificity.

(D) At all weeks of diabetes, STZ-treated mice showed pathologically elevated blood glucose of ~30 mM (p < 0.0001, n = 7). See Figure S2 for retinal *Sema3A* expression in *db/db* mice.

(E) The rise in *Sema3A* expression preceded pericyte loss as evidenced by similar levels of transcripts for pericyte-related markers platelet-derived growth factor receptor-β (*Pdgfr-β*), neuron-glial antigen 2 (*Ng2*) proteoglycan, and alpha smooth muscle actin (*α-Sma*) in STZ- and vehicle-treated mice. Data are represented as mean ± SEM.

(F–I) Equivalent vascular coverage by pericytes 8 weeks after STZ injection as depicted by pericyte-specific markers *α-Sma* (F) and *Ng2* (G) in control retinas and *α-Sma* (H) and *Ng2* (I) in STZ retinas (representative of at least three separate experiments). Scale bar = 100 μm.

(J and K) Immunofluorescence on retinal cryosections revealed that SEMA3A protein was minimally expressed in healthy retinas (J) but robustly induced by retinal ganglion cells (RGCs) in the ganglion cell layer (GCL) at 8 weeks after STZ injection (K), as confirmed by colocalization with the RGC marker βIII-tubulin (insets). Representative images of three independent experiments. Scale bar = 20 μm; inset = 10 μm.

(L and M) Laser-capture micro-dissection of the GCL from normal or diabetic mice followed by quantitative RT-PCR confirmed an ~5-fold induction of *Sema3A* in neurons in close proximity to the inner retinal vascular bed (p = 0.014, n = 3). Data are represented as mean ± SEM. Scale bar = 20 μm.

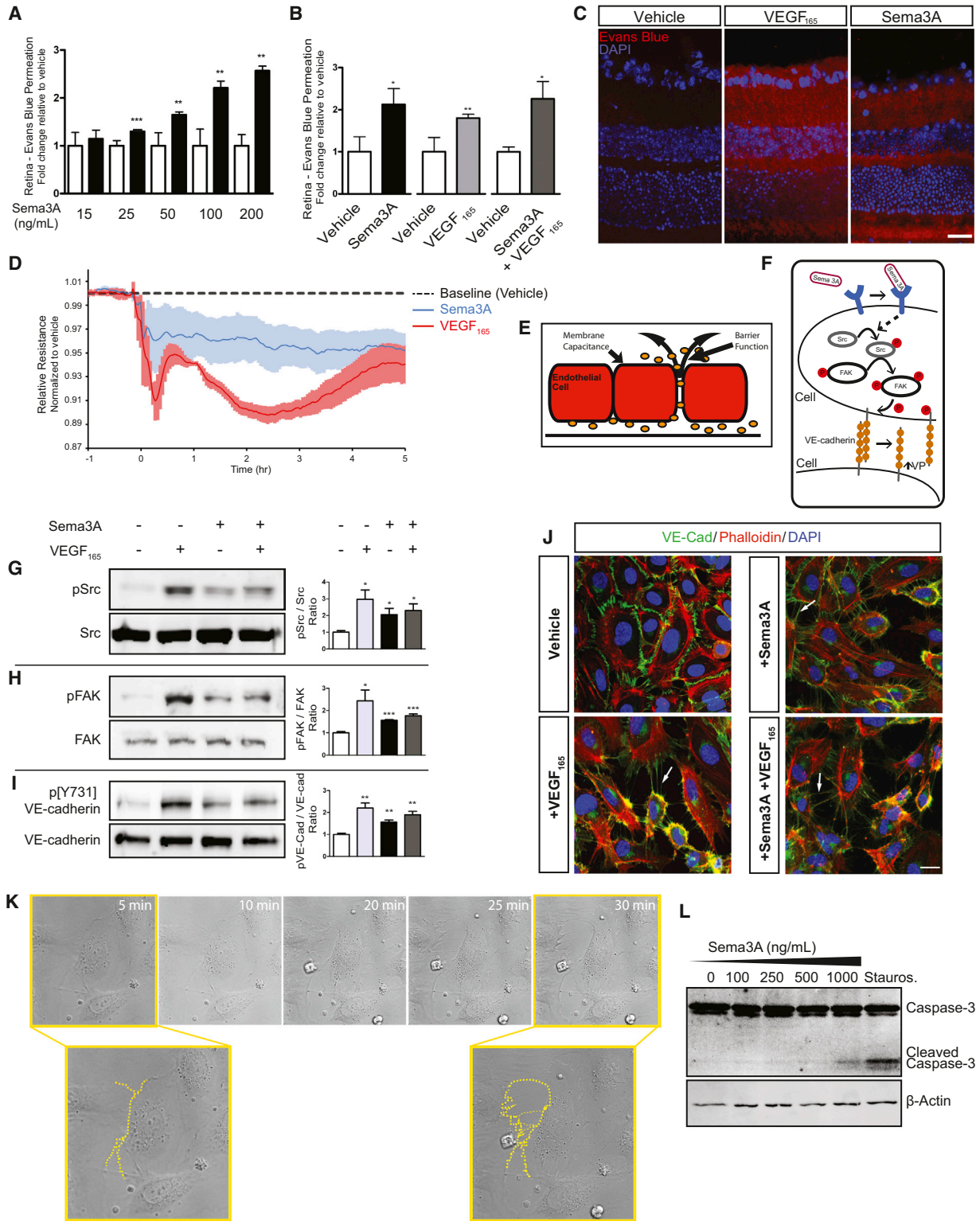

Figure 3. Retinal Barrier Function Is Compromised by SEMA3A

(A) Dose response for Sema3A-induced retinal vascular permeability (VP) as determined by Evans blue (EB) permeation (white bars are vehicle and black bars are Sema3A treated; n = 3 [9 mice] for each dose). Data are represented as mean ± SEM.

(B) Intravitreal injection of Sema3A resulted in a similar increase in retinal VP ($p < 0.01$, n = 3 [9 mice]) as observed with intravitreal administration of VEGF ($p < 0.05$, n = 3 [9 mice]) and with a combination of both Sema3A and VEGF ($p < 0.001$, n = 3 [9 mice]). Values expressed relative to vehicle injected retinas ± SEM. See also Figure S3 for wet weights of Sema3A-treated retinas.

(legend continued on next page)

et al., 2005; Schlaepfer et al., 1994) (Figure 3I). Consistent with the above data on retinal permeability (Figures 3A and 3C), we did not observe an additive or synergistic effect when stimulation of HRMECs was performed with a combination of Sema3A and VEGF, suggesting a potential eventual convergence of signaling pathways for both factors (Figures 3G–3I).

The ability of an endothelial cell to maintain intact intercellular junctions dictates the quality of barrier function. We therefore investigated changes in endothelial cell morphology secondary to Sema3A exposure. Consistent with a role in inducing vascular permeability, confocal microscopy of Sema3A-treated HRMECs revealed pronounced formation of vascular retraction fibers as determined by VE-cadherin and phalloidin staining (white arrows; Figure 3J). The retraction was similar to that observed with VEGF alone or with a combination of VEGF and Sema3A. Membrane retraction is corroborated by time-lapse imaging, and the dotted yellow lines represent the cell-cell interface of two endothelial cells (Figure 3K). While not a direct measure of cell permeability, these in vitro results highlight the morphological changes induced by Sema3A.

Importantly, at the doses employed in our study (100–200 ng/ml), Sema3A did not induce cell death or apoptosis in HRMECs, as determined by assessment of activation (cleavage) of caspase-3 (Figure 3L). These data support the role of Sema3A in mediating the breakdown of endothelial cell barrier function and further substantiate the involvement of Sema3A in diabetes-induced retinal vascular permeability.

Inhibition of Neuron-Derived SEMA3A Efficiently Reduces Pathological Vascular Permeability in T1DM

To investigate the therapeutic potential of blocking SEMA3A in diabetic retinopathy, we proceeded to inhibit it using two distinct approaches: virally delivered interference RNA or a SEMA3A trap. The magnitude of retinal vascular leakage was assessed 8 weeks after administration of STZ in adult mice. At this time point, flatmount retinas from STZ mice show elevated expression of phosphorylated VE-cadherin in lectin-stained retinal endothelial cells (Figure 4A), and animals have a significant ~57% increase in retinal vascular leakage (Figure 4B) (citrate, 1.000 ± 0.1284; STZ, 1.568 ± 0.1323, p = 0.027; n = 4 distinct experiments with a total of 12 mice).

Recent evidence suggests that retinal neurons exert an important influence on the blood vessels that perfuse them (Antonetti et al., 2012; Binet et al., 2013; Fukushima et al., 2011; Joyal et al., 2011; Kim et al., 2011; Sapieha et al., 2008). In light of the robust expression of *Sema3A* in diabetic RGCs (Figure 2), we sought to inhibit production of this guidance cue directly in RGCs using a lentiviral (Lv) vector carrying small hairpin RNAs (shRNAs) against *Sema3A* (Joyal et al., 2011). We generated Lv vectors with a VSVG capsid, which exhibits high tropism for RGCs when delivered intravitreally (Binet et al., 2013; Joyal et al., 2011; Sapieha et al., 2008) (Figure 4C). Efficiency of this approach was confirmed, as a single intravitreal injection of Lv.sh*Sema3A* at 5 weeks of life (1 week prior to STZ administration) lead to a significant (~63%) reduction in retinal *Sema3A* expression at the 8-week time point after STZ administration when all analysis was carried out (mean fold increase over control ± SEM = 0.3767 ± 0.07911; p = 0.0014, n = 3) (Figure 4D). Lv.sh*Sema3A*-mediated reduction in retinal *Sema3A* expression provoked an ~50% decrease in vascular leakage when compared to control Lv.shGFP (0.5105 ± 0.1347; p = 0.022, n = 3 distinct experiments with a total of 9 mice) (Figure 4E), thus validating the strategy of targeting *Sema3A* in neurons of the GCL to counter pathological vascular leakage in diabetes.

In order to therapeutically neutralize vitreal SEMA3A, we employed recombinant mouse soluble NRP1 (rmNRP1) as a bivalent trap for both SEMA3A and VEGF. Neuropilin-1 is a single-pass receptor with its extracellular domain subdivided into distinct subdomains of which a1a2 bind SEMA3A and b1b2 bind VEGF (Geretti et al., 2008) (Figure 4F). Intravitreal injections of rmNRP1 at 6 and 7 weeks after STZ administration lead to a ~50% reduction in retinal permeability when compared to vehicle-injected controls, as measured at 8 weeks after STZ (0.5538 ± 0.1459, p = 0.012, n = 6 distinct experiments with a total of 18 mice) (Figure 4G). This reduction was of similar magnitude to that observed with gene silencing of *Sema3A* (Figure 4E). Importantly, neutralization of VEGF with a neutralizing antibody for mouse $VEGF_{164}$ was not effective at reducing vascular permeability at this early stage of diabetes (vehicle versus anti-VEGF: 0.975 ± 0.0707; p = 0.7302; rmNRP1 versus anti-mVEGF: p = 0.035, n = 5 distinct experiments with a total of 14 mice). This is likely attributed to the fact that VEGF is not increased in diabetic retinas at this early time point (8 weeks), while *Sema3A* is robustly induced (Figure 2). Together, these data suggest that neutralization of SEMA3A in the diabetic retina is an effective strategy to reduce vasogenic edema (Figure 4H).

Conditional Knockout of *Nrp1* Prevents SEMA3A-Induced Retinal Barrier Function Breakdown

In light of NRP1 being the cognate receptor for SEMA3A, we sought to determine whether deletion of *Nrp1* protects against

(C) Confocal images of retinal sections injected with vehicle, VEGF, or Sema3A; red signal depicts leakage of Evans blue/albumin into the retina. Representative images of three independent experiments. Scale bar = 30 μm.
(D) Transendothelial resistance measured in real time by ECIS demonstrates that Sema3A effectively reduces endothelial barrier function (3.26–6 hr; 0.048 > p > 0.009; n = 3) to a level similar to that observed with VEGF (1.12–6 hr; 0.045 > p > 0.001; n = 4).
(E) ECIS measures true barrier function by assessing the resistance of the paracellular pathway between the cells.
(F–I) Working hypothesis for Sema3A-mediated vascular permeability (F). Treatment of HRMECs with either Sema3A or VEGF leads to robust phosphorylation of Src at Tyr416 (G), FAK on Tyr576 and Tyr577 (H), and the adherence junction protein VE-cadherin on Tyr731 (I). An additive or enhanced effect was not observed when simulation was performed with a combination of Sema3A and VEGF. *p < 0.05, **p < 0.01,***p < 0.001 relative to vehicle ± SEM.
(J) Confocal microscopy of Sema3A-treated HRMECs revealed formation of vascular retraction fibers as determined by VE-cadherin and phalloidin staining (white arrows); retraction was similar to that seen with VEGF alone or with a combination of VEGF and Sema3A. Scale bar = 20 μm.
(K) Membrane retraction is corroborated by time-lapse imaging, where dotted yellow lines represent the cell-cell interface.
(L) Sema3A doses employed in our study (100–200 ng/ml) did not induce cell death or apoptosis, as determined by assessment of activation of caspase-3. Representative images of three independent experiments are shown.

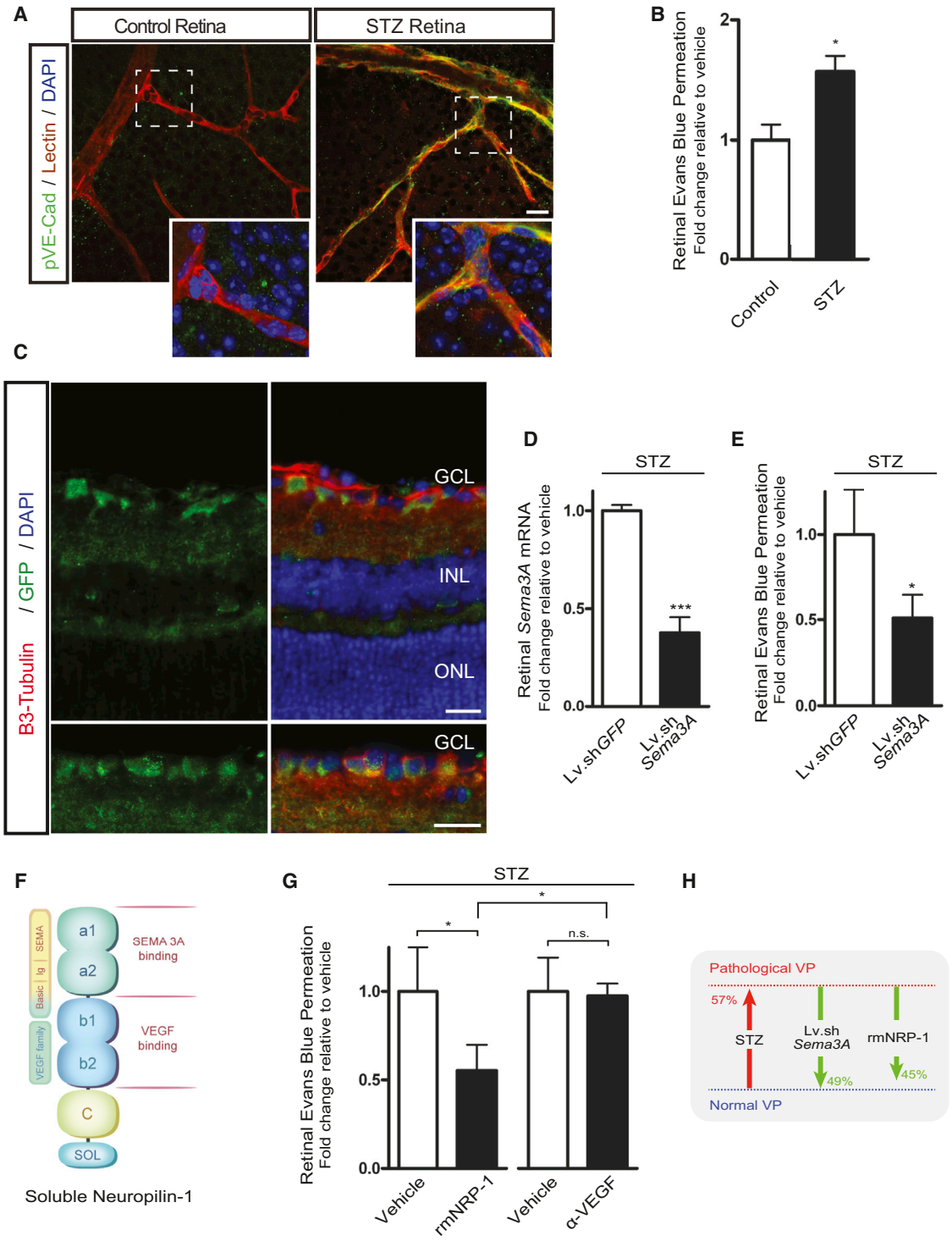

Figure 4. Targeted Silencing of Neuron-Derived *Sema3A* or Intravitreal Neutralization of SEMA3A Efficiently Reduces Diabetes-Induced Retinal Vascular Permeability

(A) Retinal flatmounts at 8 weeks following STZ-injection show elevated VE-cadherin phosphorylation (linked to higher permeability) on lectin-positive retinal vessels. Representative images of three independent experiments are shown. Scale bar = 20 μm.

(B) STZ-treated mice show a 56.8% increase in permeability ($p = 0.027$; $n = 4$ [12 mice]). Data are represented as mean ± SEM.

(C) Lentiviral vectors with a VSVG capsid exhibit high tropism for RGCs when delivered intravitreally, as depicted by a reporter Lv vector carrying GFP. Scale bar = 20 μm.

(D and E) A single intravitreal injection of Lv.sh*Sema3A* 5 weeks after induction of diabetes lead to a significant 62.3% reduction in retinal *Sema3A* expression ($p = 0.0014$, $n = 3$) (D) and provoked a proportional 49.5% decrease in vascular leakage ($p = 0.022$, $n = 3$ [9 mice]) (E). Data are represented as mean ± SEM.

(legend continued on next page)

SEMA3A-induced vascular permeability. Because systemic germline deletion of *Nrp1* is embryonic lethal (Jones et al., 2008; Kawasaki et al., 1999; Kitsukawa et al., 1997), we generated a whole-animal tamoxifen-inducible (Tam-inducible) Cre mouse ($Tg^{Cre\text{-}Esr1}$) to induce the conditional deletion of exon 2 of *Nrp1* (Figure 5A). To validate Cre recombination at the *Nrp1* locus and confirm disruption of *Nrp1* in vivo, $Tg^{Cre\text{-}Esr1}$ mice were crossed with $Nrp1^{fl/fl}$ mice (Gu et al., 2003). Progeny were given tamoxifen systemically (400 μg/mouse) over a period of 5 consecutive days at 6–9 weeks of age. This dosing regimen lead to an efficient knockout of *Nrp1* in the circulatory system, as determined by western blot (Figure 5B) and quantitative PCR (qPCR) (mean fold increase over control ± SEM = 0.07843 ± 0.03176; p = 0.0012) of heart tissue (Figure 5C), and resulted in a near complete absence of NRP1 in retinal vessels (Figure 5D). Tam-treated $Tg^{Cre\text{-}Esr1}/Nrp1^{fl/fl}$ mice did not show any difference in body weight, size, or open-field activity when compared with littermates from 4–20 weeks of age (data not shown). Importantly, Tam-treated $Tg^{Cre\text{-}Esr1}/Nrp1^{fl/fl}$ mice with disrupted retinal vascular *Nrp1* were protected against Sema3A-induced retinal vascular permeability (1.276 ± 0.2901; p = 0.36; n = 7 distinct experiments with 21 mice) (Figure 5E), while control Tam-treated $Tg^{Cre\text{-}ESR1}/Nrp1^{+/+}$ mice showed a 3-fold increase in vascular leakage in response to Sema3A (2.972 ± 0.2045; p = 0.00065; n = 3 distinct experiments with a total of 9 mice). Conversely, disruption of *Nrp1* did not influence VEGF-induced vascular retinal permeability (Tam-treated $Tg^{Cre\text{-}Esr1}/Nrp1^{fl/fl}$ vehicle versus VEGF: 1.814 ± 0.1188, p = 0.0024, n = 3 distinct experiments with a total of 9 mice; Tam-treated $Tg^{Cre\text{-}Esr1}/Nrp1^{+/+}$ vehicle versus VEGF: 1.783 ± 0.2440; p = 0.032, n = 3 distinct experiments with a total of 9 mice) (Figure 5F), suggesting that VEGF-induced retinal vascular permeability does not require NRP1. This is in accordance with previous work (Pan et al., 2007). In line with a role for NRP1 in mediating Sema3A-induced vascular permeability, knockdown of *Nrp1* in HRMECs by Lv.sh*Nrp1* prevents phosphorylation of Src, FAK, and VE-Cadherin (Figures 5G–5I). Efficiency of short hairpin RNA (sh)-mediated knockdown of *Nrp1* was validated by qPCR (Figure S4). Collectively, these data confirm that Sema3A-mediated inner blood-retinal barrier function breakdown is NRP1 dependent.

DISCUSSION

Therapeutic strategies to treat complications associated with diabetic retinopathy until recently consisted predominantly in controlling systemic metabolic deregulation (Silva et al., 2010). While laser photocoagulation and targeted treatments, such as locally administered corticosteroids and recently approved anti-VEGF therapies, are currently available, their off-target effects underscore the need to explore novel therapeutic avenues. In the present study, we provide evidence that Sema3A provokes vascular barrier breakdown in the early phases of diabetic retinopathy and ultimately precipitates DME when vascular pericyte coverage is still unperturbed. While the biological functions of semaphorins have been studied for the past 20 years (Luo et al., 1993), novel physiological roles continue to emerge (Acevedo et al., 2008; Bernard et al., 2012; Bouvrée et al., 2012; Fukushima et al., 2011; Gu et al., 2002; 2003; Guttmann-Raviv et al., 2007; Joyal et al., 2011; Kim et al., 2011; Le Guelte et al., 2012; Maione et al., 2009; Matsuoka et al., 2011; Serini et al., 2003; Suto et al., 2007). We demonstrate that in a healthy mature retina, *Sema3A* is modestly expressed, whereas in diabetes, retinal ganglion neurons, which are in intimate proximity of retinal vessels (Sapieha, 2012), significantly increase production of this classic guidance cue. Through its cognate receptor Nrp1, Sema3A provokes loosening of endothelial cell junctions and leads to vasogenic edema (Figure 5J).

Sema3A presents itself as an attractive candidate for therapeutic neutralization in adult ocular vasculopathies, given that its physiological roles are largely limited to embryogenesis. In addition, further properties that make Sema3A a noteworthy drug target are its abilitites to induce apoptosis and promote cytoskeleton remodeling (Guttmann-Raviv et al., 2007; Klagsbrun and Eichmann, 2005; Miao et al., 1999; Neufeld et al., 2012), which are both salient features of ischemic and proliferative retinopathies such as that of diabetes (Duh, 2011; Sapieha et al., 2010; Wang et al., 2012). Importantly, at the early time points in disease where levels of SEMA3A are elevated, VEGF levels remain low and relatively unchanged compared to nondiabetic controls. Given these expression kinetics and our data demonstrating that neutralization of VEGF may be ineffective in early disease, inhibition of Sema3A may be warranted in the primary phases of disease when low VEGF levels are not yet reflective of the level of pathological vascular permeability.

While the introduction of anti-VEGF therapy to attenuate neovascular age-related macular degeneration (AMD), and more recently DME, has resulted in a profound change in clinical treatment paradigms, inhibition of a molecule that plays key roles in vascular homeostasis warrants contemplation in a condition such as diabetes where vascular stability is already compromised. Hence, neutralizing Sema3A instead of currently targeted factors such vasoprotective and neuroprotective VEGF and placental growth factor (PlGF) may provide a valid therapeutic alternative for diabetic retinopathy. Exclusive neutralization of Sema3A in the early phase of diabetes would thus permit the baseline levels of VEGF present to play out their protective ocular and systemic roles (Robinson et al., 2001; Stewart, 2012). Alternatively, in later phases of disease, neutralization of Sema3A may also be sought as an adjunct to currently employed anti-VEGF therapies such as bevacizumab (Avastin), ranibizumab (Lucentis), or aflibercept (Eylea), given that both proteins seem to be present in later stages of disease and have similar effects on retinal vascular barrier function. In this regard, soluble NRP1 could be employed as a bivalent semaphorin 3A and VEGF trap, due to its intrinsic ability to bind both molecules.

(F) Vitreal SEMA3A was neutralized with a recombinant mouse (rm) soluble NRP1 protein employed as a bivalent trap for both SEMA3A and VEGF.
(G) Intravitreal injection of rmNRP1 in STZ mice at weeks 6 and 7 after induction of diabetes lead to a 48.1% reduction in retinal permeability at week 8 of diabetes (p = 0.012, n = 6 [18 mice]). Conversely, injection of a neutralizing antibody against mouse VEGF was ineffective at reducing diabetes-induced retinal permeability at this stage of disease when compared to vehicle (p = 0.7302, n = 5 [14 mice]). Values are expressed relative to vehicle-injected retinas ± SEM.
(H) Depiction of the magnitude of reversal of pathological vascular permeability with different strategies of SEMA3A neutralization.

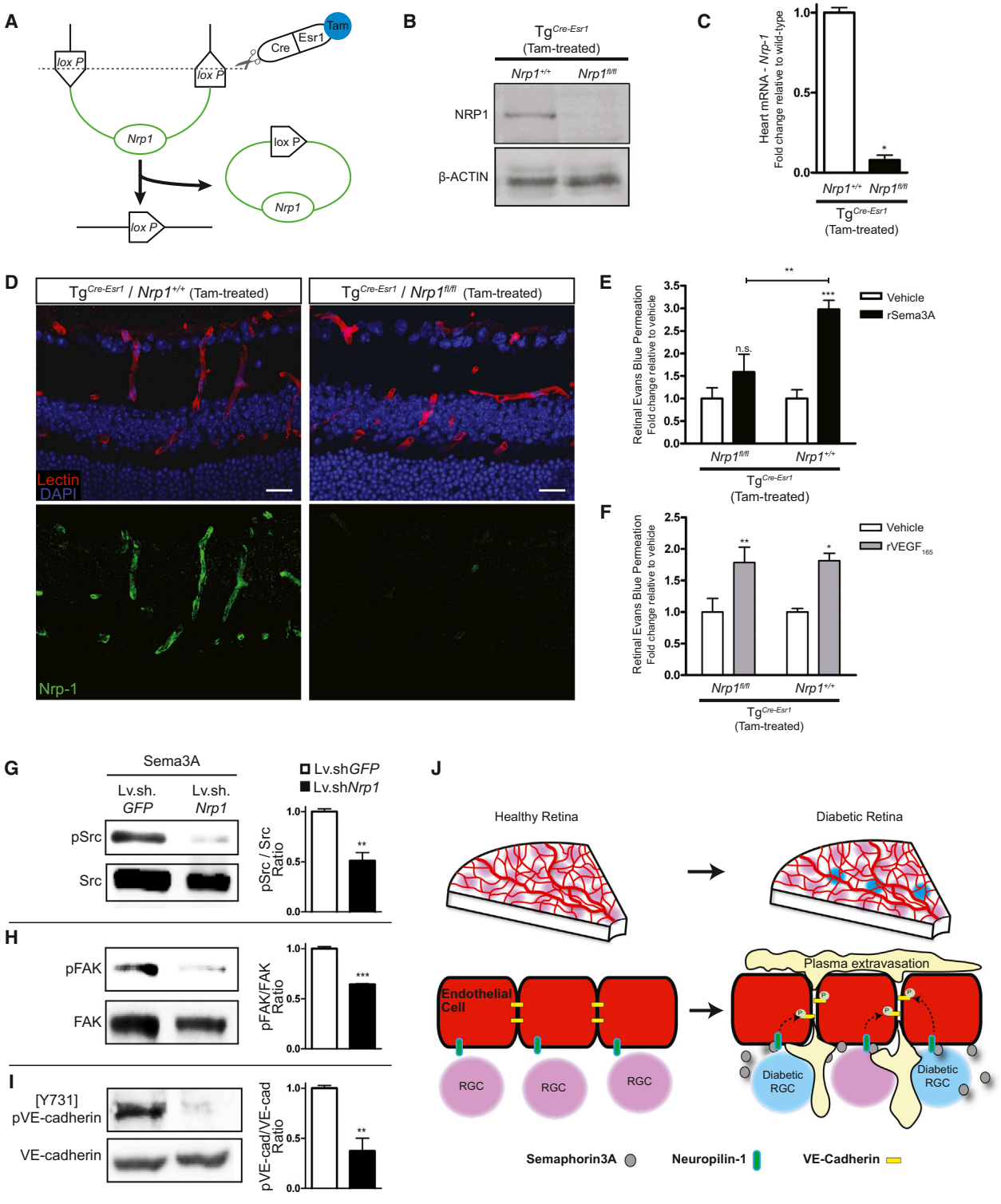

Figure 5. Conditional Knockout of *Nrp1* Prevents Sema3A-Induced Retinal Barrier Function Breakdown

Tamoxifen (Tam) was administered systemically during a 5-day period to tamoxifen-inducible *Nrp1* floxed B6 mice ($Tg^{Cre\text{-}Esr1}/Nrp1^{fl/fl}$).

(A) Graphic depiction of the inducible Cre-loxP system where estrogen receptor 1 (Esr1) forms a complex with Cre recombinase; Tam, when available, binds the Cre-Esr1 complex, allowing its nuclear translocation and the subsequent recombination and/or excision of the floxed target gene *Nrp1*.

(B) Efficiency of *Nrp1* deletion by CRE-Esr1 recombinase is evidenced by decreased Nrp-1 protein.

(C) Similarly, *Nrp-1* mRNA transcript is reduced as determined in heart tissue ($p = 0.0012$; $n = 2$). Data are represented as mean ± SEM.

(D) Immunofluorescence in retinal cryosections reveals the efficiency of Tam-induced knockdown of *Nrp1* in lectin-stained retinal vessels.

(legend continued on next page)

Using Tam-treated $Tg^{Cre\text{-}Esr1}/Nrp1^{fl/fl}$ to conditionally delete *Nrp1* in mature animals, we provide in vivo evidence for the role of this receptor in mediating the effects of SEMA3A on vascular barrier function breakdown. NRP1 also acts as a coreceptor for $VEGF_{165}$, increasing its affinity toward VEGF receptor-2 (VEGFR-2), thus enhancing VEGFR-2-mediated chemotaxis, growth of endothelial cells, and angiogenesis (Miao et al., 2000; Soker et al., 1998; 2002). However, in our hands, the effects of VEGF on vascular permeability do not seem to require NRP1, since Tam-treated $Tg^{Cre\text{-}Esr1}/Nrp1^{fl/fl}$ mice showed a magnitude of retinal edema identical to that of control Tam-treated $Tg^{Cre\text{-}Esr1}/Nrp1^{+/+}$ mice, secondary to elevated VEGF administration. This is consistent with previous studies demonstrating that blocking the VEGF or Sema3A binding sites of NRP1 with distinct monoclonal antibodies had no effect on VEGF-induced vascular permeability (Pan et al., 2007). It is important to note that it was previously elegantly demonstrated that selective deletion of *Nrp1* in the endothelium of adult mice renders them resistant to both Sema3A- and VEGF-mediated intradermal vascular permeability (Acevedo et al., 2008). Interestingly, the authors also noted that mice that received systemic treatment with a monoclonal antibody directed against Nrp1, known to inhibit VEGF binding, potently inhibited Sema3A-induced permeability yet had little effect on VEGF-induced permeability. These discrepancies highlight the context-dependent contribution of Nrp1 to VEGF-mediated vascular permeability. It is likely that the point of signaling convergence lies downstream of Nrp1, given that costimulation of ECs with both VEGF and SEMA3A does not enhance permeability beyond levels noted when each is applied independently.

Because there is a certain mechanistic overlap in the etiologies of several ocular vasculopathies, such as neovascular AMD, diabetic retinopathy, retinal vein occlusions, and retinopathy of prematurity, treatment paradigms such as anti-VEGFs are being used or explored for more than one ocular vasculopathy. Similarly, Sema3A neutralization may be useful for treating vessel leakage and edema associated with neovascular AMD (Yancopoulos, 2010). Moreover, we have previously demonstrated in a model of oxygen-induced retinopathy (Smith et al., 1994) that in late stages of pathological retinal neovascularization, neuronal-derived SEMA3A forms a repulsive barrier that hinders normal revascularization by misdirecting vessels away from the ischemic retina (Joyal et al., 2011). Hence, inhibition of Sema3A could potentially simultaneously benefit the two main pathognomonic features of DR, i.e., barrier function deterioration and pathological preretinal neovascularization, which separately can lead to loss of vision in diabetes.

By studying neurovascular interplay in diabetes, we obtained insight into a fundamental neurovascular mechanism that mediates pathological barrier function breakdown in diabetic retinopathy. Collectively, our study identifies a therapeutic target, Sema3A, which may be involved beyond DME in diseases in which elevated vascular permeability is a contributing factor, such as neovascular AMD, retinopathy of prematurity, cancer, and stroke.

EXPERIMENTAL PROCEDURES

For detailed experimental procedures, please see Supplemental Information.

Human Samples

The study conforms to the tenets of the Declaration of Helsinki, and approval of the human clinical protocol and informed consent was obtained from the Maisonneuve-Rosemont Hospital (HMR) ethics committee (Ref. CER: 10059).

Vitrectomy

All patients previously diagnosed with DME were followed and operated by a single vitreoretinal surgeon (F.A.R.). Control patients were undergoing surgical treatment for nonvascular pathology (ERM or MH) by the same surgeon (F.A.R.).

Animals

All studies were performed according to the Association for Research in Vision and Ophthalmology (ARVO) Statement for the Use of Animals in Ophthalmic and Vision Research. Tamoxifen-inducible (Tam-inducible) Cre mice ($Tg^{Cre\text{-}Esr1}$; no. 004682) and neuropilin-1 floxed mice ($Nrp1^{tm2Ddg}$/J; no. 005247) were purchased from The Jackson Laboratory.

Streptozotocin Mouse Model

C57BL/6J mice (6–7 weeks old) were weighed, and their baseline glycemia was measured (Accu-Chek, Roche). Mice were injected intraperitoneally with streptozotocin (Sigma-Aldrich) for 5 consecutive days at 55 mg/kg.

Laser-Capture Microdissection

Eyes were enucleated from 14-week-old adult C57BL/6J that had been diabetic for 8 weeks and flash frozen in optimal cutting temperature compound (OCT). Sections of 12 μm were dissected with a Zeiss Observer microscope equipped with a PALM MicroBeam device for laser-capture microdissection.

Assessment of Sema3A Levels by ELISA

Vitreous samples were frozen on dry ice immediately after biopsy and stored at −80°C. ELISA was performed according to manufacturer's instructions (Uscn Life Science).

Western Blotting, Immunofluorescence, Real-Time PCR Analysis, and Antibodies

Please see Supplemental Information.

Evans Blue Permeation Assay

Retinal EB permeation was performed with modifications as described in (Xu et al., 2001). EB was injected at 45 mg/kg intravenously, and it was allowed to circulate for 2 hr prior to retinal extraction. Evans blue permeation was quantified by fluorimetry (620 nm max absorbance, 740 nm minimum absorbance

(E) In absence of NRP1, intravitreally administered Sema3A did not increase vascular leakage ($p = 0.36$; $n = 7$ [21 mice]), while Tam-treated $Tg^{Cre\text{-}ESR1}/Nrp1^{+/+}$ controls show 3-fold higher vascular leakage ($p = 0.00065$; $n = 3$ [9 mice]). Data are represented as mean ± SEM.
(F) Conversely, disruption of *Nrp1* did not influence VEGF-induced vascular retinal permeability ($p = 0.0024$; $n = 3$ [9 mice]), suggesting that VEGF-induced retinal vascular leakage is independent of NRP1 as previously reported. Data are represented as mean ± SEM.
(G–I) In vitro knockdown of *Nrp1* in HRMECs by Lv.sh*Nrp1* prevents phosphorylation of Src ($p = 0.004$; $n = 3$) (G), FAK ($p = 0.0002$; $n = 3$) (H), and VE-cadherin ($p = 0.0081$; $n = 3$) (I). Data are represented as mean ± SEM. See Figure S4 for efficacy of sh*Nrp1*-mediated knockdown of Nrp1.
(J) Graphic depiction of the main findings of the study. In a healthy mature retina, levels of *Sema3A* are low, whereas in diabetes, retinal ganglion neurons in intimate proximity of retinal vessels significantly increase their production. Through NRP1, Sema3A provokes loosening of endothelial cell junctions and leads to vasogenic edema.

background) with a TECAN Infinite M1000 PRO. EBP (measured in ul / [g × hr]) is calculated as (EB [ug] / wet retinal weight [g]) / (plasma EB [ug/ul] × circulation time [hr]). Evans blue permeation was expressed relative to controls.

Electric Cell-Substrate Impedance Sensing Assay

Real-time analysis of transendothelial electric resistance was performed by plating HUVECs onto 8W10E+ standard 8-well arrays (Applied BioPhysics) at a density of 10^5 cells per well. Please see Supplemental Information.

Preparation of Lentivirus

Viral vectors were produced as previously described by us (Binet et al., 2013; Joyal et al., 2011). Please see Supplemental Information.

Soluble Recombinant NRP1 and Mouse anti-VEGF

STZ-treated diabetic C57BL/6J mice were intravitreally injected with rmNRP1 from plasmid (Mamluk et al., 2002) or R&D Systems at 6 and 7 weeks after STZ administration. Specific mouse anti-VEGF was purchased from R&D Systems (AF-493-NA), and 1 μl was injected at 80 ug/ml. Retinal Evans blue permeation assay was performed at 8 weeks after STZ treatment as described above.

Statistical Analyses

We used Student's t test and ANOVA, where appropriate, to compare the different groups; $p < 0.05$ was considered statistically different. For ELISA, a nonparametric Mann-Whitney test was used. Results were expressed as median and interquartile range (IQR: 25%, 75%).

SUPPLEMENTAL INFORMATION

Supplemental Information includes Supplemental Experimental Procedures and four figures and can be found with this article online at http://dx.doi.org/10.1016/j.cmet.2013.09.003.

AUTHOR CONTRIBUTIONS

P.S. and A.C. conceived and designed the experiments. A.C., N.T., C.M., K.M., F.A.R., A.D., C.P., E.L., N.S., F. Binet, D.L., V.D.G., and F. Beaudoin performed the experiments. A.C., N.T., C.M., K.M., C.P., E.L., A.D., F.A.R., and P.S. analyzed the data. F.A.R. performed all vitreous biopsies. A.C., N.T., C.M., and P.S. assembled the figures. P.S. wrote the manuscript.

ACKNOWLEDGMENTS

The University of Montreal, Hospital Maisonneuve-Rosemont and P.S. have filed a patent pertaining to the results presented in the paper. This work was supported by operating grants to P.S. from the Canadian Diabetes Association (OG-3-11-3329-PS), the Canadian Institutes of Health Research (221478), the Foundation Fighting Blindness Canada, and Les Fonds de Recherche en Ophtalmologie de l'Université de Montréal. P.S. holds a Canada Research Chair in Retinal Cell Biology and The Alcon Research Institute Young Investigator Award. A.C. is supported by scholarships from the Réseau de Recherche en Sante de la Vision du Québec (RRSV). N.S. and F.B. hold a Fonds de la Recherche en Santé du Québec (FRSQ) postdoctoral fellowship. F. Beaudoin is supported by the The Whitearn Foundation. We thank Wei Li for the illustration in Figures 2 and 4. We thank Lois E.H. Smith for assessment of *Sema3A* in *db/db* mice. We also give special thanks to Aouatef Benlemmouden for coordinating patients for clinical sampling of vitreous.

Received: April 8, 2013
Revised: July 20, 2013
Accepted: August 23, 2013
Published: October 1, 2013

REFERENCES

Acevedo, L.M., Barillas, S., Weis, S.M., Göthert, J.R., and Cheresh, D.A. (2008). Semaphorin 3A suppresses VEGF-mediated angiogenesis yet acts as a vascular permeability factor. Blood *111*, 2674–2680.

Antonetti, D.A., Klein, R., and Gardner, T.W. (2012). Diabetic retinopathy. N. Engl. J. Med. *366*, 1227–1239.

Appleton, B.A., Wu, P., Maloney, J., Yin, J., Liang, W.C., Stawicki, S., Mortara, K., Bowman, K.K., Elliott, J.M., Desmarais, W., et al. (2007). Structural studies of neuropilin/antibody complexes provide insights into semaphorin and VEGF binding. EMBO J. *26*, 4902–4912.

Barber, A.J., Lieth, E., Khin, S.A., Antonetti, D.A., Buchanan, A.G., and Gardner, T.W. (1998). Neural apoptosis in the retina during experimental and human diabetes. Early onset and effect of insulin. J. Clin. Invest. *102*, 783–791.

Barber, A.J., Antonetti, D.A., Kern, T.S., Reiter, C.E., Soans, R.S., Krady, J.K., Levison, S.W., Gardner, T.W., and Bronson, S.K. (2005). The Ins2Akita mouse as a model of early retinal complications in diabetes. Invest. Ophthalmol. Vis. Sci. *46*, 2210–2218.

Bernard, F., Moreau-Fauvarque, C., Heitz-Marchaland, C., Zagar, Y., Dumas, L., Fouquet, S., Lee, X., Shao, Z., Mi, S., and Chédotal, A. (2012). Role of transmembrane semaphorin Sema6A in oligodendrocyte differentiation and myelination. Glia *60*, 1590–1604.

Binet, F., Mawambo, G., Sitaras, N., Tetreault, N., Lapalme, E., Favret, S., Cerani, A., Leboeuf, D., Tremblay, S., Rezende, F., et al. (2013). Neuronal ER stress impedes myeloid-cell-induced vascular regeneration through IRE1α degradation of netrin-1. Cell Metab. *17*, 353–371.

Bouvrée, K., Brunet, I., Del Toro, R., Gordon, E., Prahst, C., Cristofaro, B., Mathivet, T., Xu, Y., Soueid, J., Fortuna, V., et al. (2012). Semaphorin3A, Neuropilin-1, and PlexinA1 are required for lymphatic valve formation. Circ. Res. *111*, 437–445.

Cheung, N., and Wong, T.Y. (2008). Diabetic retinopathy and systemic vascular complications. Prog. Retin. Eye Res. *27*, 161–176.

Duh, E.J. (2011). Sema 3A resists retinal revascularization. Blood *117*, 5785–5786.

Eliceiri, B.P., Paul, R., Schwartzberg, P.L., Hood, J.D., Leng, J., and Cheresh, D.A. (1999). Selective requirement for Src kinases during VEGF-induced angiogenesis and vascular permeability. Mol. Cell *4*, 915–924.

Foxton, R.H., Finkelstein, A., Vijay, S., Dahlmann-Noor, A., Khaw, P.T., Morgan, J.E., Shima, D.T., and Ng, Y.S. (2013). VEGF-A is necessary and sufficient for retinal neuroprotection in models of experimental glaucoma. Am. J. Pathol. *182*, 1379–1390.

Fukushima, Y., Okada, M., Kataoka, H., Hirashima, M., Yoshida, Y., Mann, F., Gomi, F., Nishida, K., Nishikawa, S., and Uemura, A. (2011). Sema3E-PlexinD1 signaling selectively suppresses disoriented angiogenesis in ischemic retinopathy in mice. J. Clin. Invest. *121*, 1974–1985.

Gastinger, M.J., Kunselman, A.R., Conboy, E.E., Bronson, S.K., and Barber, A.J. (2008). Dendrite remodeling and other abnormalities in the retinal ganglion cells of Ins2 Akita diabetic mice. Invest. Ophthalmol. Vis. Sci. *49*, 2635–2642.

Gelfand, M.V., Hong, S., and Gu, C. (2009). Guidance from above: common cues direct distinct signaling outcomes in vascular and neural patterning. Trends Cell Biol. *19*, 99–110.

Geretti, E., Shimizu, A., and Klagsbrun, M. (2008). Neuropilin structure governs VEGF and semaphorin binding and regulates angiogenesis. Angiogenesis *11*, 31–39.

Gluzman-Poltorak, Z., Cohen, T., Shibuya, M., and Neufeld, G. (2001). Vascular endothelial growth factor receptor-1 and neuropilin-2 form complexes. J. Biol. Chem. *276*, 18688–18694.

Gu, C., Limberg, B.J., Whitaker, G.B., Perman, B., Leahy, D.J., Rosenbaum, J.S., Ginty, D.D., and Kolodkin, A.L. (2002). Characterization of neuropilin-1 structural features that confer binding to semaphorin 3A and vascular endothelial growth factor 165. J. Biol. Chem. *277*, 18069–18076.

Gu, C., Rodriguez, E.R., Reimert, D.V., Shu, T., Fritzsch, B., Richards, L.J., Kolodkin, A.L., and Ginty, D.D. (2003). Neuropilin-1 conveys semaphorin and VEGF signaling during neural and cardiovascular development. Dev. Cell *5*, 45–57.

Guttmann-Raviv, N., Shraga-Heled, N., Varshavsky, A., Guimaraes-Sternberg, C., Kessler, O., and Neufeld, G. (2007). Semaphorin-3A and semaphorin-3F work together to repel endothelial cells and to inhibit their survival by induction of apoptosis. J. Biol. Chem. *282*, 26294–26305.

Hunter, T. (1987). A tail of two src's: mutatis mutandis. Cell *49*, 1–4.

Jones, E.A., Yuan, L., Breant, C., Watts, R.J., and Eichmann, A. (2008). Separating genetic and hemodynamic defects in neuropilin 1 knockout embryos. Development *135*, 2479–2488.

Joyal, J.-S., Sitaras, N., Binet, F., Rivera, J.C., Stahl, A., Zaniolo, K., Shao, Z., Polosa, A., Zhu, T., Hamel, D., et al. (2011). Ischemic neurons prevent vascular regeneration of neural tissue by secreting semaphorin 3A. Blood *117*, 6024–6035.

Kawasaki, T., Kitsukawa, T., Bekku, Y., Matsuda, Y., Sanbo, M., Yagi, T., and Fujisawa, H. (1999). A requirement for neuropilin-1 in embryonic vessel formation. Development *126*, 4895–4902.

Kempen, J.H., O'Colmain, B.J., Leske, M.C., Haffner, S.M., Klein, R., Moss, S.E., Taylor, H.R., and Hamman, R.F.; Eye Diseases Prevalence Research Group. (2004). The prevalence of diabetic retinopathy among adults in the United States. Arch. Ophthalmol. *122*, 552–563.

Kern, T.S., and Engerman, R.L. (1996). Capillary lesions develop in retina rather than cerebral cortex in diabetes and experimental galactosemia. Arch. Ophthalmol. *114*, 306–310.

Kim, J., Oh, W.J., Gaiano, N., Yoshida, Y., and Gu, C. (2011). Semaphorin 3E-Plexin-D1 signaling regulates VEGF function in developmental angiogenesis via a feedback mechanism. Genes Dev. *25*, 1399–1411.

Kitsukawa, T., Shimizu, M., Sanbo, M., Hirata, T., Taniguchi, M., Bekku, Y., Yagi, T., and Fujisawa, H. (1997). Neuropilin-semaphorin III/D-mediated chemorepulsive signals play a crucial role in peripheral nerve projection in mice. Neuron *19*, 995–1005.

Klagsbrun, M., and Eichmann, A. (2005). A role for axon guidance receptors and ligands in blood vessel development and tumor angiogenesis. Cytokine Growth Factor Rev. *16*, 535–548.

Klagsbrun, M., Takashima, S., and Mamluk, R. (2002). The role of neuropilin in vascular and tumor biology. Adv. Exp. Med. Biol. *515*, 33–48.

Klebanov, O., Nitzan, A., Raz, D., Barzilai, A., and Solomon, A.S. (2009). Upregulation of Semaphorin 3A and the associated biochemical and cellular events in a rat model of retinal detachment. Graefes Arch. Clin. Exp. Ophthalmol. *247*, 73–86.

Koppel, A.M., and Raper, J.A. (1998). Collapsin-1 covalently dimerizes, and dimerization is necessary for collapsing activity. J. Biol. Chem. *273*, 15708–15713.

Le Guelte, A., Galan-Moya, E.M., Dwyer, J., Treps, L., Kettler, G., Hebda, J.K., Dubois, S., Auffray, C., Chneiweiss, H., Bidere, N., and Gavard, J. (2012). Semaphorin 3A elevates endothelial cell permeability through PP2A inactivation. J. Cell Sci. *125*, 4137–4146.

Lee, P., Goishi, K., Davidson, A.J., Mannix, R., Zon, L., and Klagsbrun, M. (2002). Neuropilin-1 is required for vascular development and is a mediator of VEGF-dependent angiogenesis in zebrafish. Proc. Natl. Acad. Sci. USA *99*, 10470–10475.

Luo, Y., Raible, D., and Raper, J.A. (1993). Collapsin: a protein in brain that induces the collapse and paralysis of neuronal growth cones. Cell *75*, 217–227.

Maione, F., Molla, F., Meda, C., Latini, R., Zentilin, L., Giacca, M., Seano, G., Serini, G., Bussolino, F., and Giraudo, E. (2009). Semaphorin 3A is an endogenous angiogenesis inhibitor that blocks tumor growth and normalizes tumor vasculature in transgenic mouse models. J. Clin. Invest. *119*, 3356–3372.

Mamluk, R., Gechtman, Z., Kutcher, M.E., Gasiunas, N., Gallagher, J., and Klagsbrun, M. (2002). Neuropilin-1 binds vascular endothelial growth factor 165, placenta growth factor-2, and heparin via its b1b2 domain. J. Biol. Chem. *277*, 24818–24825.

Martin, D.F., Maguire, M.G., Ying, G.S., Grunwald, J.E., Fine, S.L., Jaffe, G.J., and Jaffe, G.J.; CATT Research Group. (2011). Ranibizumab and bevacizumab for neovascular age-related macular degeneration. N. Engl. J. Med. *364*, 1897–1908.

Martin, D.F., Maguire, M.G., Fine, S.L., Ying, G.S., Jaffe, G.J., Grunwald, J.E., Toth, C., Redford, M., and Ferris, F.L., 3rd.; Comparison of Age-related Macular Degeneration Treatments Trials (CATT) Research Group. (2012). Ranibizumab and bevacizumab for treatment of neovascular age-related macular degeneration: two-year results. Ophthalmology *119*, 1388–1398.

Matsuoka, R.L., Nguyen-Ba-Charvet, K.T., Parray, A., Badea, T.C., Chédotal, A., and Kolodkin, A.L. (2011). Transmembrane semaphorin signalling controls laminar stratification in the mammalian retina. Nature *470*, 259–263.

Miao, H.Q., Soker, S., Feiner, L., Alonso, J.L., Raper, J.A., and Klagsbrun, M. (1999). Neuropilin-1 mediates collapsin-1/semaphorin III inhibition of endothelial cell motility: functional competition of collapsin-1 and vascular endothelial growth factor-165. J. Cell Biol. *146*, 233–242.

Miao, H.Q., Lee, P., Lin, H., Soker, S., and Klagsbrun, M. (2000). Neuropilin-1 expression by tumor cells promotes tumor angiogenesis and progression. FASEB J. *14*, 2532–2539.

Mima, A., Qi, W., Hiraoka-Yamomoto, J., Park, K., Matsumoto, M., Kitada, M., Li, Q., Mizutani, K., Yu, E., Shimada, T., et al. (2012). Retinal not systemic oxidative and inflammatory stress correlated with VEGF expression in rodent models of insulin resistance and diabetes. Invest. Ophthalmol. Vis. Sci. *53*, 8424–8432.

Moss, S.E., Klein, R., and Klein, B.E. (1998). The 14-year incidence of visual loss in a diabetic population. Ophthalmology *105*, 998–1003.

Murakami, M., Nguyen, L.T., Zhuang, Z.W., Moodie, K.L., Carmeliet, P., Stan, R.V., and Simons, M. (2008). The FGF system has a key role in regulating vascular integrity. J. Clin. Invest. *118*, 3355–3366.

Neufeld, G., Sabag, A.D., Rabinovicz, N., and Kessler, O. (2012). Semaphorins in angiogenesis and tumor progression. Cold Spring Harb Perspect Med *2*, a006718.

Pan, Q., Chanthery, Y., Liang, W.C., Stawicki, S., Mak, J., Rathore, N., Tong, R.K., Kowalski, J., Yee, S.F., Pacheco, G., et al. (2007). Blocking neuropilin-1 function has an additive effect with anti-VEGF to inhibit tumor growth. Cancer Cell *11*, 53–67.

Potter, M.D., Barbero, S., and Cheresh, D.A. (2005). Tyrosine phosphorylation of VE-cadherin prevents binding of p120- and beta-catenin and maintains the cellular mesenchymal state. J. Biol. Chem. *280*, 31906–31912.

Robinson, G.S., Ju, M., Shih, S.C., Xu, X., McMahon, G., Caldwell, R.B., and Smith, L.E. (2001). Nonvascular role for VEGF: VEGFR-1, 2 activity is critical for neural retinal development. FASEB J. *15*, 1215–1217.

Saint-Geniez, M., Maharaj, A.S., Walshe, T.E., Tucker, B.A., Sekiyama, E., Kurihara, T., Darland, D.C., Young, M.J., and D'Amore, P.A. (2008). Endogenous VEGF is required for visual function: evidence for a survival role on müller cells and photoreceptors. PLoS ONE *3*, e3554.

Sapieha, P. (2012). Eyeing central neurons in vascular growth and reparative angiogenesis. Blood *120*, 2182–2194.

Sapieha, P., Sirinyan, M., Hamel, D., Zaniolo, K., Joyal, J.-S., Cho, J.-H., Honoré, J.-C., Kermorvant-Duchemin, E., Varma, D.R., Tremblay, S., et al. (2008). The succinate receptor GPR91 in neurons has a major role in retinal angiogenesis. Nat. Med. *14*, 1067–1076.

Sapieha, P., Hamel, D., Shao, Z., Rivera, J.C., Zaniolo, K., Joyal, J.S., and Chemtob, S. (2010). Proliferative retinopathies: angiogenesis that blinds. Int. J. Biochem. Cell Biol. *42*, 5–12.

Sapieha, P., Chen, J., Stahl, A., Seaward, M.R., Favazza, T.L., Juan, A.M., Hatton, C.J., Joyal, J.S., Krah, N.M., Dennison, R.J., et al. (2012). Omega-3 polyunsaturated fatty acids preserve retinal function in type 2 diabetic mice. Nutr Diabetes *2*, e36.

Scheppke, L., Aguilar, E., Gariano, R.F., Jacobson, R., Hood, J., Doukas, J., Cao, J., Noronha, G., Yee, S., Weis, S., et al. (2008). Retinal vascular permeability suppression by topical application of a novel VEGFR2/Src kinase inhibitor in mice and rabbits. J. Clin. Invest. *118*, 2337–2346.

Schlaepfer, D.D., Hanks, S.K., Hunter, T., and van der Geer, P. (1994). Integrin-mediated signal transduction linked to Ras pathway by GRB2 binding to focal adhesion kinase. Nature *372*, 786–791.

Serini, G., Valdembri, D., Zanivan, S., Morterra, G., Burkhardt, C., Caccavari, F., Zammataro, L., Primo, L., Tamagnone, L., Logan, M., et al. (2003). Class 3 semaphorins control vascular morphogenesis by inhibiting integrin function. Nature *424*, 391–397.

Silva, P.S., Cavallerano, J.D., Sun, J.K., Aiello, L.M., and Aiello, L.P. (2010). Effect of systemic medications on onset and progression of diabetic retinopathy. Nat. Rev. Endocrinol. *6*, 494–508.

Smith, L.E., Wesolowski, E., McLellan, A., Kostyk, S.K., D'Amato, R., Sullivan, R., and D'Amore, P.A. (1994). Oxygen-induced retinopathy in the mouse. Invest. Ophthalmol. Vis. Sci. *35*, 101–111.

Soker, S., Takashima, S., Miao, H.Q., Neufeld, G., and Klagsbrun, M. (1998). Neuropilin-1 is expressed by endothelial and tumor cells as an isoform-specific receptor for vascular endothelial growth factor. Cell *92*, 735–745.

Soker, S., Miao, H.Q., Nomi, M., Takashima, S., and Klagsbrun, M. (2002). VEGF165 mediates formation of complexes containing VEGFR-2 and neuropilin-1 that enhance VEGF165-receptor binding. J. Cell. Biochem. *85*, 357–368.

Stahl, A., Connor, K.M., Sapieha, P., Chen, J., Dennison, R.J., Krah, N.M., Seaward, M.R., Willett, K.L., Aderman, C.M., Guerin, K.I., et al. (2010). The mouse retina as an angiogenesis model. Invest. Ophthalmol. Vis. Sci. *51*, 2813–2826.

Stewart, M.W. (2012). The expanding role of vascular endothelial growth factor inhibitors in ophthalmology. Mayo Clin. Proc. *87*, 77–88.

Suto, F., Tsuboi, M., Kamiya, H., Mizuno, H., Kiyama, Y., Komai, S., Shimizu, M., Sanbo, M., Yagi, T., Hiromi, Y., et al. (2007). Interactions between plexin-A2, plexin-A4, and semaphorin 6A control lamina-restricted projection of hippocampal mossy fibers. Neuron *53*, 535–547.

Takahashi, T., Fournier, A., Nakamura, F., Wang, L.H., Murakami, Y., Kalb, R.G., Fujisawa, H., and Strittmatter, S.M. (1999). Plexin-neuropilin-1 complexes form functional semaphorin-3A receptors. Cell *99*, 59–69.

Vieira, J.M., Schwarz, Q., and Ruhrberg, C. (2007). Role of the neuropilin ligands VEGF164 and SEMA3A in neuronal and vascular patterning in the mouse. Novartis Found. Symp. *283*, 230–235, discussion 235–241.

Wang, S., Park, J.K., and Duh, E.J. (2012). Novel targets against retinal angiogenesis in diabetic retinopathy. Curr. Diab. Rep. *12*, 355–363.

Xu, Q., Qaum, T., and Adamis, A.P. (2001). Sensitive blood-retinal barrier breakdown quantitation using Evans blue. Invest. Ophthalmol. Vis. Sci. *42*, 789–794.

Yancopoulos, G.D. (2010). Clinical application of therapies targeting VEGF. Cell *143*, 13–16.